Cancer Imaging (2012) **12,** 452–463
DOI: 10.1102/1470-7330.2012.0041

www.e-med.org.uk

REVIEW

Diffusion magnetic resonance imaging of chest tumors

A.A.K. Abdel Razek

Department of Diagnostic Radiology, Mansoura Faculty of Medicine, Mansoura, Egypt

Corresponding address: Ahmed Abdel Khalek Abdel Razek, Department of Diagnostic Radiology, Mansoura Faculty of Medicine, Mansoura, 35512, Egypt.
Email: arazek@mans.edu.eg

Date accepted for publication 23 August 2012

Abstract

This review provides an overview of the current status of the published data on diffusion magnetic resonance (MR) imaging of chest tumors. Diffusion MR imaging is a non-invasive imaging technique that measures the differences in water mobility in different tissue microstructures and quantifies them based on the apparent diffusion coefficient. Diffusion MR imaging has been used for the characterization, grading and staging of lung cancer as well as for differentiating central tumors from post-obstructive consolidation. In addition, this technique helps in differentiating malignant from benign pulmonary and mediastinal tumors as well as in the characterization of pleural mesothelioma and effusion. Diffusion MR imaging can be incorporated into routine morphological MR imaging to improve radiologist confidence in image interpretation and to provide functional assessments of chest tumors during the same examination. Diffusion MR imaging could be used in the future as a functional imaging technique for tumors of the chest.

Keywords: *Diffusion; MR imaging; chest; lung cancer; mediastinal; lymph node; pleura; tumor.*

Introduction

Metabolic imaging of the chest with [^{18}F]fluorodeoxyglucose (FDG)-positron emission tomography (PET), or combined with computed tomography (CT), relies on physiologic parameters, such as glucose metabolism, to assist in differentiating between malignant and benign pulmonary or nodal lesions[1]. However, it is still constrained by the current resolution limits for small nodal metastasis (5 mm)[2], which are associated with false-positive and false-negative results, and the exposure of patients to ionizing radiation[1–3]. Cross-sectional imaging techniques, such as CT and MR imaging, rely on morphologic criteria for the assessment of pulmonary and mediastinal tumors. Morphologic findings would be helpful in differentiating benign and malignant pulmonary lesions when they have typical features; however, there is considerable overlap in morphologic presentation, and differentiation may be challenging in many cases. MR imaging has now entered the stage as a radiation-free alternative to CT for certain indications. Current MR imaging techniques, such as perfusion MR imaging, enable functional imaging of the chest. The addition of diffusion-weighted MR imaging to routine MR imaging may lead to the provision of better thoracic protocols in which both morphologic and functional sequences are combined, allowing for the comprehensive assessment of chest tumors in a single MR examination[4,5].

Diffusion MR imaging is well established as a diagnostic tool in the primary assessment of acute stroke[6]. However, in the last few years, several extracranial applications of diffusion MR imaging have been developed. Major applications have been described in the diagnosis, detection, characterization, prognosis before treatment, and evaluation and follow-up after treatment of tumoral lesions in the abdomen, breast, and head and neck region[7–10]. The recent technical advances in fast MR imaging have greatly enhanced the clinical value of MR imaging of the chest. These developments include faster imaging techniques with echoplanar imaging and parallel imaging, high performance gradients and phased-array multichannel surface coils[11–14]. To date, there have been several reports describing the application of diffusion MR imaging in lung cancer[15–39], mediastinal masses[40–44] and pleural lesions[45–47].

This paper is available online at http://www.cancerimaging.org. In the event of a change in the URL address, please use the DOI provided to locate the paper.

1470-7330/12/000001 + 12

This review provides an overview of the current status of the published data on diffusion MR imaging of the chest tumors.

Principles of diffusion MR imaging

Diffusion MR imaging generates image contrast based on the microscopic mobility of water. Diffusion is the random thermal motion of gaseous or liquid molecules, and MR imaging can detect signal changes caused by positional changes of molecules at this microscopic scale. Diffusion in a homogeneous medium is described as having a Gaussian distribution. In biological tissue, there is a high probability that water molecules interact with structures, such as cell membranes and macromolecules, that reduce or impede their motion. Water exchange occurs between intracellular and extracellular compartments and is based on the shape of the extracellular space and tissue cellularity, which affect diffusion[6–8]. In solid malignant lesions, the extravascular extracellular space is relatively diminished compared with the intracellular space due to an increased number of cells, cellular pleomorphism, large cell volume and neoangiogenic vessels disorganized in a chaotic structure. This increased microstructural density will restrict random water molecule movement. In contrast, the extravascular extracellular space is relatively enlarged compared with the intracellular space in inflammation and infection due to the presence of interstitial edema and in necrosis due to the absence of organized tissues. Thus, the reduced interactions with cell membranes facilitate random water molecule movement[9–13].

Diffusion-weighted MR imaging was obtained by application of symmetric pairs of equally weighted diffusion-sensitizing gradients about the 180° refocusing pulse of a spin echo T2-weighted sequence. Static water molecules develop additional phase incoherencies from the application of the first diffusion gradient, but these incoherencies are eliminated by the application of the second gradient, resulting in no additional net loss of signal (aside from normal T2 decay). However, mobile water is not completely rephased by the second gradient due to movement to a different microenvironment during the application of the first gradient, so that a subsequent reduction in signal intensity is observed[6–8]. The signal intensity reduction on diffusion MR imaging can be quantified by calculating the apparent diffusion coefficient (ADC), which depends largely on the presence of barriers to diffusion within the water microenvironment. The ADC values are calculated from a series of diffusion MR images at different *b* values. The *b* value is the product of the gyromagnetic ratio, the strength of the diffusion-sensitizing gradients, the duration of the gradient pulse and the time interval between gradient pairs[11–13].

Areas of restricted diffusion (e.g., highly cellular malignant tumors) are bright on diffusion-weighted images acquired using a high *b* value and dark on the ADC map (i.e., representing a relatively low ADC value), as opposed to the areas of unrestricted diffusion (e.g., edema or fluid), which demonstrate low signal intensity on diffusion-weighted images acquired using a high *b* value and brightness on the ADC map (i.e., representing a relatively high ADC value). Also, it is quite possible that unrestricted diffusion still presents with high signal on higher *b* values, due to T2-shine through[11–13].

Techniques

Diffusion MR imaging of the chest is technically challenging and not always feasible due to obvious shortcomings, such as motion artifacts related to breathing and heart and vascular pulsation and susceptibility artifacts associated with air–tissue interfaces. The applications of diffusion MR imaging of the chest have increased considerably in the last few years due to recent technologic improvements, such as more powerful gradients and phased-array coils and the development of fast imaging techniques, such as echo planar imaging (EPI) and parallel imaging[11,12].

Acquisition

Sequence

EPI is the most frequent diffusion-weighted imaging sequence. Single-shot spin echo EPI has a short acquisition time. The image quality using this technique, however, can be degraded due to low resolution, chemical shift artifacts, susceptibility artifacts, and geometric distortion. Different strategies have been proposed to diminish EPI-related artifacts, such as segmentation of the echo train length of the EPI acquisition in different shots; the application of motion correction techniques, such as navigation echoes; and the use of the periodically rotated overlapping parallel lines with enhanced reconstruction acquisition (PROPELLER), which is less sensitive to motion artifacts and the use of parallel imaging. Furthermore, improvements in gradient systems with reduced eddy current effects have allowed for faster EPI readout, which can decrease geometric distortions[11–13]. Imaging may be performed during a single breath hold, which attempts to freeze motion, or during free breathing with multiple signal acquisitions to reduce the effects of motion. Image acquisition during free breathing may also be combined with respiratory and/or cardiac triggering[13]. The use of a respiratory trigger improves the quality of diffusion MR imaging sequences compared with those using breath holding[11]. The use of a cardiac trigger is also useful for avoiding pulsation artifacts, but it is not always necessary, except in cases of lesions located immediately around the heart or in dedicated cardiac acquisitions, as they are time consuming[11].

Several non-EPI techniques, including conventional spin echo and stimulated echo and fast spin echo, have

been used for diffusion-weighted imaging of the chest. These techniques have better resolution and are less degraded by susceptibility artifacts and less prone to geometric distortion. Distortion and fat suppression is much better on turbo spin echo imaging, causing the larger chemical shift effect to disappear[11,12].

b value

The choice of *b* values is most likely the pivotal issue of diffusion MR imaging. Diffusion-weighted imaging is typically performed with at least two *b* values to allow for the calculation of the ADC value. Imaging with low *b* values provides higher signal-to-noise ratios but with less diffusion weighting. As the *b* value increases, sensitivity to the effects of diffusion increases, but there is greater image distortion. However, the use of even greater *b* values may be beneficial. The optimal *b* values for diffusion MR imaging of the chest have not yet been determined. With current state-of-the-art magnets, a *b* value of 1000 s/mm^2 can be obtained. The suggested *b* value is greater than 500 s/mm^2 to avoid the effects of perfusion. In addition, a *b* value less than 1000 s/mm^2 is recommended for a better signal-to-noise ratio[11–15].

Fat suppression

The use of fat suppression is mandatory in diffusion MR imaging of the chest because fat signals usually overlap on the studied anatomy. Diffusion MR imaging with short tau inversion recovery (STIR) has been most commonly used in the chest, in sequences such as diffusion-weighted imaging with background suppression (DWIBS). To overcome the limited signal-to-noise ratio of these sequences, spectral fat suppression techniques, such as spectral presaturation inversion recovery (SPIR) and spectral selection attenuated inversion recovery (SPAIR), have been included in diffusion MR imaging sequences[11].

Three Tesla

Although most of the reported applications of diffusion MR imaging of the chest have been performed with 1.5-T magnets, the use of higher-field magnets, such as 3 T, has been advocated due to the associated signal improvement. The acquisition problems inherent to diffusion MR imaging increase with 3-T magnets, due to higher magnetic field variation and susceptibility artifacts, which can be overcome using the appropriately higher strength of the gradient systems in combination with parallel imaging and advanced fat suppression sequences. Gill et al.[45] recently reported the first clinical series of diffusion MR imaging performed using a 3-T magnet with adequate technical tuning; diffusion-weighted imaging of the chest is feasible with 3-T magnets[11].

Table 1 shows the recommended imaging protocol for diffusion-weighted MR imaging of the chest.

Calculation

Monocompartmental fit

Calculation of the ADC value is the most common method used to quantitatively analyze diffusion MR imaging. The ADC value is usually calculated by the slope of the line of the natural logarithm of signal intensity versus *b* values. In effect, this yields a monocompartmental fit for the raw signal intensity data[6–8]. A region of interest (ROI) is drawn around the lesion or its components (e.g., necrotic core, enhancing periphery) on multiple scans, and the average ADC value of that volume is computed. There is a lack of standardization in ROI analysis, which is prone to errors because it is operator dependent. The number and size of ROIs vary from series to series. There is also no consensus regarding whether it is more appropriate to use the mean or minimal ADC value. This limitation of the ADC has led to the development of the alternative ADC measures described below[1–12].

Bicompartmental model

The bicompartmental model for the analysis of pulmonary lesions improves lesional characterization by using the parameter *D* (diffusion coefficient) instead of the ADC calculation, which is usually greater than *D* due to perfusion effects. The use of an intravoxel incoherent motion (IVIM) diffusion MR imaging sequence with several *b* values allows us to separate the two components of the diffusion signal decay, one of which is due to perfusion at low *b* values and the other of which is the true diffusion that occurs with *b* values greater than 100 s/mm^2[11].

Evaluation

Parametric ADC maps

A parametric ADC map is a graphical representation of changes in the ADC on a voxel-to-voxel basis. Specifically, such a map displays those voxels that have increased in ADCs, decreased in ADCs, or shown no change in the ADCs in different colors to enable instantaneous visual representation of changes within the lesion. Such a map makes it easier to assess the overall change in diffusion within a lesion and to identify particular areas that may have deviated from the overall trend[11,12].

ADC histogram

Histogram analysis of ADC values is a post-processing method used to analyze heterogeneous lung cancer. In this approach, the ROI of a lesion is identified on multiple scans, and a plot of the number of voxels at each ADC value is depicted as a histogram[10–12].

Table 1 **Recommended imaging protocol for diffusion MR imaging of the chest**

Pulse sequence	Single-shot spin echo EPI
Coil	Phased-array surface coil
Fat suppression	Chemical shift selective (CHESS) fat suppression
Field of view	35–40 cm
b value	1000 s/mm^2
Parallel imaging	Acceleration factor of 2
Number of slices	24–30
Repetition time (TR)	5000 ms
Echo time (TE)	50 ms
Slice thickness	5–8 mm
Number of excitations	6

Clinical applications

Lung cancer

Differentiating lung cancer from benign lung masses, non-small cell lung cancer (NSCLC) from small cell lung cancer (SCLC), and low-grade from high-grade malignancies and determining the staging of lung cancer are essential for treatment planning[4,5]. Diffusion MR imaging can be useful for the characterization and grading of lung cancer[14–27] (Fig. 1) as well as the assessment of associated lymph nodes and distant metastases[30–36]. Table 2 provides an overview of studies of diffusion MR imaging of lung cancer.

Detection of pulmonary nodules

Regier et al.[14] reported that diffusion MR imaging is more sensitive than multidetector CT in the detection of solid pulmonary nodules. For diffusion MR imaging, a sensitivity of 86.4% was calculated for nodules ranging from 6 to 9 mm and 97% for nodules large than 10 mm. In contrast, only 43.8% of lesions larger than 5 mm were detected on multidetector CT.

Differentiation of lung cancer from benign pulmonary masses

Diffusion MR imaging has been used for differentiating between lung cancer and benign pulmonary masses. Lung cancer is characterized by increased cellularity, larger nuclei with more abundant macromolecular proteins, a larger nuclear/cytoplasmic ratio and less extracellular space relative to normal tissue. Because of these characteristics, the diffusion of water molecules in malignant tumors is restricted, resulting in decreased ADC values (Fig. 1). In contrast, benign pulmonary masses are characterized by less cellularity and more extracellular space, with relatively less impeded diffusion[13–20].

In 2011, Tondo et al.[20] reported that there were statistically significant differences ($P = 0.05$) between the ADC values of benign and malignant lesions. Using an ADC value of 1.25×10^{-3} mm^2/s as a threshold, they were able to differentiate malignant from benign lesions with 91% diagnostic accuracy, 90% sensitivity and 100% specificity. In 2010, Liu et al.[16] reported that the mean ADC value of benign lesions ($1.65 \pm 0.42 \times 10^{-3}$ mm^2/s) was statistically greater ($P = 0.001$) than that of malignant tumors ($1.26 \pm 0.32 \times 10^{-3}$ mm^2/s). The optimal threshold ADC value for the differentiation of malignant

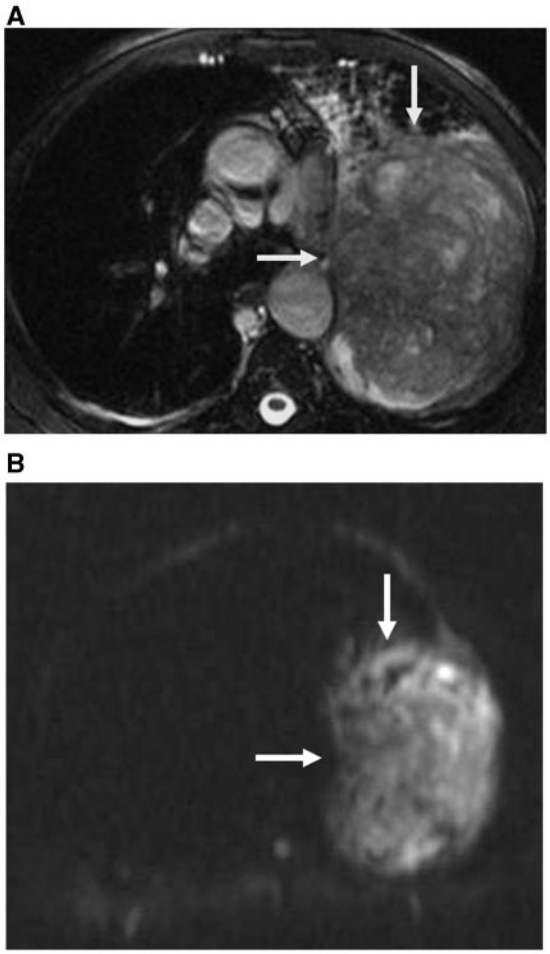

Figure 1 **NSCLC. (A) Axial true fast imaging with steady state precession (FISP) shows peripheral lung cancer (arrows). (B) Diffusion MR image shows restricted diffusion of the mass (arrows) with a low ADC value (0.89×10^{-3} mm^2/s).**

Table 2 **Overview of studies on diffusion MR imaging of lung cancer**

Study	Journal	Year	Purpose	*b* value	Findings
Regier[14]	J Med Imaging Radiat Oncol	2011	Detection of pulmonary nodules	500	Significant difference ($P<0.05$) in ADC between benign and malignant lesions
Tondo[20]	Radiol Med	2011	Cancer vs benign	1000	Significant differences ($P<0.05$) in ADC between benign and malignant lesions
Liu[16]	Eur Radiol	2010	Cancer vs benign	800	Diffusion-weighted imaging can differentiate between benign and malignant lung nodules
Uto[19]	Radiology	2009	Cancer vs benign	1000	Diffusion-weighted imaging can differentiate between benign and malignant lung nodules
Satoh[17]	Am J Roentgenol	2008	Cancer vs benign	1000	Signal intensity can differentiate malignant from benign nodules on diffusion-weighted imaging
Mori[18]	J Thorac Oncol	2008	Cancer vs benign	1000	Diffusion-weighted imaging also reduces the rate of false-positive lesions compared with PET
Matobi[15]	Radiology	2007	Subtypes of lung cancer	577	The ADC of adenocarcinoma is significantly higher than that of squamous cell carcinoma or large-cell carcinoma
Kanauchi[25]	Eur J Cardiothorac Surg	2009	Invasiveness of NSCLC	1000	Diffusion-weighted imaging can predict tumor invasiveness
Obha[22]	J Thorac Cardiovasc Surg	2009	NSCLC	1000	Diffusion-weighted imaging is similar to PET in distinguishing NSCLC from benign pulmonary nodules
Regier[27]	Eur J Radiol	2011	NSCLC	500	ADC value correlated with uptake on PET/CT
Koyama[24]	Eur Radiol	2010	Subtypes of adenocarcinoma	500	Diffusion-weighted imaging shows no significant differences regarding subtype classification
Tanaka[23]	J Thorac Imaging	2009	Adenocarcinoma	1000	Strong signal intensity on diffusion-weighted imaging is significantly greater in advanced BAC and non-BAC than in BAC
Baysal[28]	Magn Reson Imaging	2009	Cancer vs collapse	1000	ADC of central lung carcinoma is lower than post-obstructive consolidations
Qi[29]	Eur Radiol	2009	Cancer vs collapse	500	Combined ADC and T2-weighted images are superior to CT in differentiating lung cancer from collapse
Pauls[33]	Eur J Radiol	2012	N staging of NSCLC	800	Diffusion-weighted imaging might be beneficial in the detection of very small nodes
Ohno[34]	Radiology	2011	N staging of NSCLC	1000	STIR is better than diffusion-weighted imaging and PET/CT for the detection of metastatic lymph nodes from NSCLC
Nakayama[32]	J Comput Assist Tomogr	2010	N staging of NSCLC	1000	Diffusion-weighted imaging enables differentiation of nodal metastasis from reactive nodes
Hasegawa[31]	J Thorac Imaging	2008	N staging of NSCLC	1000	Diffusion-weighted imaging can exclude metastatic lymph nodes from NSCLC
Nomari[30]	J Thorac Cardiovasc Surg	2008	N staging of NSCLC	1000	Diffusion-weighted imaging can be used in place of PET/CT for N staging of NSCLC
Ohno[39]	Am J Roentgenol	2012	Response of NSCLC to chemotherapy	1000	ADC better predicts the response to chemotherapy of NSCLC than PET/CT
Yabuuchi[38]	Radiology	2011	Response of NSCLC to chemotherapy	1000	Correlation between ADC change and final NSCLC size reduction after chemotherapy
Okuma[37]	Br J Radiol	2009	Response of lung cancer to RFA	1000	ADC can predict the response to radiofrequency ablation of lung cancer

tumors from benign lesions was 1.4×10^{-3} mm^2/s, with sensitivity and specificity of 83.3% and 74.1%, respectively. In 2008, Satoh et al.[17] reported that the ADC value accurately differentiated benign from malignant pulmonary nodules larger than 5 mm, with an area under the curve of 0.80. Small metastases and some non-solid adenocarcinomas were predominantly hypointense on diffusion-weighted images with high *b* values. Granulomas and active inflammatory and fibrous nodules occasionally showed low signal intensity, similar to malignancies. In 2008, Mori et al.[18] reported that the ADC value of lung cancer was significantly different from that of benign pulmonary masses. In 2009, Obha et al.[22] suggested that diffusion MR imaging is equivalent to PET for distinguishing NSCLC from benign pulmonary nodules.

It is difficult to compare the results from the referenced series because of the different diffusion MR imaging sequences performed and the different qualitative and quantitative assessment methods. As a general rule, diffusion MR imaging of pulmonary nodules obtains adequate results in the differentiation of benign from malignant nodules. Of the limited data available comparing diffusion MR imaging with FDG-PET, both techniques perform equally in pulmonary lesion characterization with similar limitations, although diffusion MR imaging tends to provide fewer false-positive results related mainly to benign inflammatory lesions[11–13].

Differentiation of SCLC from NSCLC

Mortality rates and the success of therapeutic approaches depend on the histologic type of lung cancer[3,24]. There is wide variability in the ADC values of different types of lung cancer among different studies. In 2007, Matoba et al.[15] applied diffusion MR imaging with a split acquisition of fast spin echo signals for diffusion imaging (SPLICE) sequences for the tissue characterization of lung cancer, with a *b* value of 68/577 s/mm^2. They reported that the ADC value for well-differentiated adenocarcinoma ($2.12 \pm 0.6 \times 10^{-3}$ mm^2/s) was significantly different ($P \leq 0.05$) from that of large-cell carcinoma ($1.30 \pm 0.4 \times 10^{-3}$ mm^2/s) and small cell carcinoma ($2.09 \pm 0.3 \times 10^{-3}$ mm^2/s). The ADC values of well-differentiated adenocarcinoma appeared to be greater than those of other histologic types ($P \leq 0.05$). In 2010, Lui et al.[16] reported that there was significant difference ($P \leq 0.007$) between the ADC values of SCLC ($1.064 \pm 0.196 \times 10^{-3}$ mm^2/s) and NSCLC ($1.321 \pm 0.335 \times 10^{-3}$ mm^2/s). The differences in ADC values might reflect differences in histopathologic features: SCLC generally has enlarged cells, and the tumor cellularity seems to be relatively high causing the lower reported ADC values in SCLC. There may be insufficient spread among the distributions to differentiate the tumor types in many patients. The discrepancy of ADC values among different studies might be attributable to different pulse sequences and different applied *b* values as well as to different methods of calculating ADC values. Further studies are required to evaluate the potential of diffusion MR imaging for differentiating subtypes of lung carcinomas.

Characterization of subtypes of adenocarcinoma

The classification of subtypes of adenocarcinoma, including bronchioloalveolar carcinoma (BAC), is important because the prognosis is different according to the subtype[23,24]. In 2009, Tanaka et al.[23] reported that both the moderate and strong signal intensities on diffusion MR imaging were significantly greater in advanced BAC (79.2%) and non-advanced BAC (88.9%) than in BAC (38.5%). Tumors with strong signal intensity on diffusion MR imaging were judged as invasive forms, with sensitivity of 97% and specificity of 76.9%. In 2010, Koyama et al.[24] added that there were no significant differences in the ADC values of subtypes of adenocarcinoma of lung cancer. The potential reason for this discrepancy between the results might be the different *b* values, number of excitations, respiratory triggering and breath-holding methods.

Grading of NSCLC

Differentiation of low- and high-grade NSCLC is essential as prognosis and mortality rates depend on the grading of the cancer[1,3,4]. The ADC of well-differentiated adenocarcinoma is significantly greater than that of moderately and poorly differentiated squamous cell carcinomas and adenocarcinomas ($P = 0.05$). The ADCs of well-differentiated adenocarcinomas with hypocellularity seem to be greater than those of other lung cancers of different histologic types. The ADC value of lung cancer is correlated well with tumor cellularity ($P = 0.02$)[16]. There was a significant difference in the ADC values of poorly versus well to moderately differentiated lung cancers ($P = 0.03$). The ADC value of lung cancer can be considered a new prognostic parameter[26]. The changes in the ADC are inversely correlated with changes in tissue cellularity: a low ADC value indicates areas of restricted diffusion in highly cellular areas, whereas a high ADC value indicates areas of diffusion in less cellular areas. The difference in cellularity may reflect the tumor's histologic composition and biological aggressiveness[13,14].

Invasiveness of NSCLC

Determining the invasiveness of NSCLC is essential for treatment planning[25]. Limited surgery should be avoided with invasive tumors. There is a positive correlation between invasive lung cancer and the ADC value ($P = 0.001$). Diffusion MR imaging may be a useful method for predicting tumor invasiveness in clinical stage 1A NSCLC. The sensitivity of diffusion MR

imaging for the prediction of tumor invasiveness is 90%; its specificity is 81%[25].

Correlation of ADC values of lung cancer with prognostic parameters

In 2011, Abdel Razek et al.[26] reported that there was a correlation between the ADC value and prognostic parameters of lung cancer. The ADC value of lung cancer is correlated with tumor grade ($r = -0.48$) and with metastatic mediastinal nodes ($r = -0.42$). In 2011, Regier et al.[27] added that there was a correlation between the ADC value and standardized uptake value (SUV) on FDG-PET/CT in NSCLC. The significant inverse correlation of these two quantitative imaging approaches demonstrates the association of metabolic activity with tumor cellularity. Therefore, diffusion MR imaging with ADC measurement might represent a new prognostic marker for NSCLC.

Differentiating lung cancer from post-obstructive consolidation

Patients with central lung cancer frequently present with peripheral lung collapse or post-obstructive pneumonia. Both findings make it difficult to differentiate central tumors from surrounding lung consolidation on CT scans or routine MR imaging. However, FDG-PET/CT scanning already has a dominant role regarding cancer delineation within atelectatic lungs. Exact knowledge of the tumor extension is of crucial importance, especially in patients scheduled for radiotherapy. The ADC value can be considered as a useful parameter to differentiate between central lung cancer and accompanying post-obstructive consolidation. In 2009, Baysal et al.[28] reported that the mean ADC value for the mass of central lung cancer ($1.83 \pm 0.75 \times 10^{-3}\,mm^2/s$) was significantly lower ($P = 0.003$) than that of post-obstructive consolidation ($2.50 \pm 0.76 \times 10^{-3}\,mm^2/s$). In 2009, Qi et al.[29] added that using a combination of T2-weighted images and diffusion-weighted images was superior to bolus CT or T2-weighted imaging alone for differentiating lung cancer from post-obstructive collapse, with a sensitivity of 88%.

N staging

In patients with NSCLC, lymph node staging plays a pivotal role as accurate nodal staging is essential for choosing the appropriate treatment strategy for patients with lung cancer[30,31]. CT is the imaging modality of choice in the evaluation of patients with suspected lung cancer, but it has limited sensitivity and specificity for the assessment of lymph node involvement. Over the last few years, FDG-PET and integrated FDG-PET/CT have been demonstrated to be highly sensitive, even in lymph nodes smaller than 1 cm. The main disadvantage of PET and PET/CT is the large number of false-positive results in patients with concurrent inflammatory lymphadenitis; moreover, PET and PET/CT are not as widely available as MR imaging[30–33]. NSCLC metastatic lymph nodes have lower ADC values than reactive or inflammatory lymph nodes[26].

It has been suggested diffusion MR imaging could be used in the future in the place of PET/CT for the N staging of NSCLC. Diffusion MR imaging is more accurate than PET/CT for the diagnosis of non-metastatic lymph nodes because of fewer false-positives with the former. The cut-off ADC value used to differentiate metastatic from non-metastatic lymph nodes in patients with NSCLC is $1.63 \times 10^{-3}\,mm^2/s$, with an accuracy of 0.89[30]. Diffusion MR imaging can be used for the diagnosis of metastatic lymph nodes in patients with NSCLC with a high degree of accuracy (95%)[31]. The mean ADC value in metastatic lymph nodes in NSCLC is less than that in nodes without metastases ($P = 0.001$) and similar to that in primary lesions, in which movement is limited due to high cellularity. There was no significant difference ($P > 0.05$) between the quantitative analyses of diffusion-weighted MR images and STIR MR images[32]. PET/CT has a greater tendency to overstage (higher number of false-positives) than MR imaging, which gives a higher number of false-negatives. MR imaging, with or without diffusion MR imaging, shows moderate correlation with PET/CT[33]. The detectable size of a metastatic thoracic lymph node with the current available technology is approximately 4–5 mm for both diffusion MR imaging and PET/CT. Therefore, lymph node dissection may not be less common for patients with N0 stage diagnosed by diffusion MR imaging or PET/CT because node metastases less than this size are not uncommon[13]. In contrast, in 2012, Ohno et al.[34] reported that the sensitivity of STIR turbo spin echo imaging (77.4%) for the detection of metastatic mediastinal lymph nodes in patients with NSCLC was significantly higher than that of diffusion-weighted imaging (71.0%, $P = 0.03$) or of FDG-PET/CT (69.9%, $P = 0.02$).

M staging

Whole-body diffusion MR imaging can be used for M-stage assessment in patients with NSCLC with an accuracy (81.8%) as good as that of integrated PET/CT; in addition, when whole-body diffusion MR imaging is adopted as an adjunct to whole-body MR imaging without whole-body diffusion MR imaging, the diagnostic accuracy of whole-body MR examination can be improved[35]. Whole-body diffusion MR imaging can be used for bone metastasis assessment in NSCLC patients as accurately as bone scintigraphy and/or PET/CT. The specificity (93.7%) and accuracy (93.9%) with whole-body MR imaging with diffusion MR imaging are significantly greater than those with bone scintigraphy or PET/CT ($P = 0.05$)[36]. Standardization of sequences for bone metastasis assessment by whole-body diffusion MR

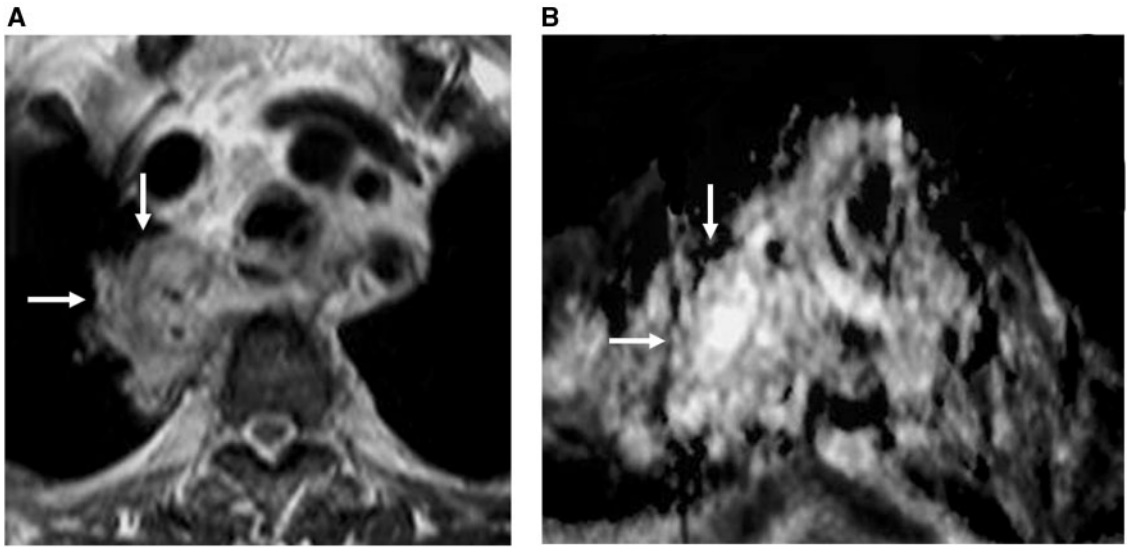

Figure 2 **Lung cancer after radiotherapy. (A) Axial T2-weighted image shows mass of mixed signal intensity (arrows) after radiotherapy. (B) ADC map shows free diffusion of the mass (arrows) with a high ADC value (2.34×10^{-3} mm^2/s) denoting post-radiation changes without residual tumor.**

imaging and improvement of MR technology for whole-body examination are necessary for better results in the future.

Prediction of treatment response and monitoring of patients with lung cancer after therapy

Other potential applications of diffusion MR imaging in lung cancer, which still need to be explored fully, are monitoring the treatment response after chemotherapy or radiation, distinguishing post-therapeutic changes (Fig. 2) from residual active tumors, and detecting recurrent cancer. Diffusion MR imaging has also been used in other organs to predict the response to a cancer treatment before and soon after therapy, but this approach must still be investigated for lung cancer. In the same vein, Okuma et al.[37] prospectively evaluated 17 patients with 20 malignant lung lesions who underwent CT-guided radiofrequency ablation. Diffusion MR imaging with ADC calculation was performed immediately before and 3 days after treatment. The post-treatment ADCs of the lesions without local progression were significantly greater than those of the lesions with local progression. However, this difference could not be demonstrated for the pretreatment ADC quantification[13]. To be validated as a biomarker for treatment response, studies correlating ADC changes with response to treatment are needed (response to biotherapies, evaluation of anticancer therapy) as well as, perhaps, radiotherapy planning.

In 2011, Yabuuchi et al.[38] studied 28 patients with NSCLC who underwent chemotherapy. The ADC value was calculated. There was a significant correlation between early ADC changes and the final rate of reduction in tumor size ($r^2 = -0.41$, $P = 0.00025$). The median progression-free survival for the group with a good increase in the ADC was 12.1 months, and that for the group with a stable or decreased ADC was 6.67 months ($P = 0.021$). Thus, the ADC seems to be a promising tool for monitoring the early response to or predicting the prognosis after chemotherapy for NSCLC. In 2012, Ohno et al.[39] added that diffusion MR imaging may have greater potential than FDG-PET/CT for the prediction of tumor response to therapy before chemoradiotherapy in NSCLC patients, by distinguishing between partial responders and non-responders (stable or progressive disease). The area under the curve for the ADC (AUC = 0.84) was significantly larger than that for SUV_{max} (AUC = 0.64). The application of feasible threshold values resulted in the specificity (44.4%) and accuracy (76.6%) of diffusion MR imaging becoming significantly greater than with PET/CT (specificity of 11.1% and accuracy of 67.2%).

Mediastinal and pleural lesions

The differentiation of malignant mediastinal masses and lymph nodes from benign mediastinal lesions as well as the differentiation of subtypes of mesothelioma and pleural effusion are essential for treatment planning, and they are of prognostic value. Diffusion MR imaging could be useful for the characterization of mediastinal masses and lymph nodes as well as the subtyping of pleural mesothelioma and effusion. Table 3 provides an overview of studies of diffusion MR imaging of mediastinal and pleural lesions.

Table 3 **Overview of studies on diffusion MR imaging of mediastinal and pleural tumors**

Study	Journal	Year	Purpose	*b* value (s/mm^2)	Findings
Abdel Razek[42]	Eur J Radiol	2012	Mediastinal mass	600	Significant differences ($P<0.001$) in ADC of benign and malignant lesions in children
Gümüştaş[41]	Eur Radiol	2011	Mediastinal mass	1000	Diffusion-weighted imaging can differentiate malignant from benign mediastinal tumors
Abdel Razek[40]	J Magn Reson Imaging	2009	Mediastinal mass	600	Diffusion-weighted imaging helps in the grading of mediastinal malignancy
Kosucu[43]	J Magn Reson Imaging	2009	Mediastinal LN	400	Signal intensity can differentiate malignant from benign lymph nodes on diffusion-weighted imaging
Abdel Razek[44]	Magn Reson Imaging	2011	Mediastinal LN	600	Diffusion-weighted imaging helps in the characterization of mediastinal lymph nodes
Cohen[49]	Radiology	2012	Malignant pleural disease	1000	Diffusion-weighted imaging is a promising tool for differentiating malignant pleural disease from benign lesions
Gill[45]	Am J Roentgenol	2009	Pleural Mesothelioma	750	ADC of epithelioid mesothelioma is higher than that of sarcomatoid mesothelioma

Mediastinal tumor

The differentiation of malignant mediastinal tumors from benign tumors in adults and children is essential for treatment planning. In adults, the ADC value of malignant mediastinal tumors ($1.09 \pm 0.25 \times 10^{-3}\,mm^2/s$) is significantly different ($P = 0.001$) from that of benign tumors ($2.38 \pm 0.65 \times 10^{-3}\,mm^2/s$)[40]. The cut-off ADC value of $\leq 1.39 \times 10^{-3}\,mm^2/s$ indicates a malignant lesion with a sensitivity of 95% and specificity of 87%[41] (Fig. 3). In children, the ADC value of malignant mediastinal tumors ($0.91 \pm 0.17 \times 10^{-3}\,mm^2/s$) is significantly different ($P = 0.001$) from that of benign tumors ($1.8 \pm 0.33 \times 10^{-3}\,mm^2/s$). The cut-off ADC value used in differentiating malignant and benign mediastinal tumors in children is $1.2 \times 10^{-3}\,mm^2/s$ with an accuracy of 93%[42]. Benign tumors, such as thymolipomas, exhibit low ADC values due to high fat content. In addition, some malignancies may reveal unrestricted diffusion with high ADC values due to less cellularity and more free fluid within the tumors, with subsequent free diffusion. The ADC value is a promising non-invasive parameter for the grading mediastinal malignancies[40–42].

Mediastinal lymphadenopathy

Determination of the mediastinal lymph nodes and the distinction between benign and malignant nodes are essential for therapy planning. Metastatic lymph nodes are usually more hypointense than benign lymph nodes, and benign lymph nodes are usually hyperintense on the calculated ADC map at a *b* value of 0 and $400\,mm^2/s$. The ADC value is significantly lower ($P = 0.0005$) in metastatic nodes ($1.01 \pm 0.02 \times 10^{-3}\,mm^2/s$) than in benign lymph nodes ($1.51 \pm 0.07 \times 10^{-3}\,mm^2/s$)[43]. The calculated ADC value of malignant mediastinal lymphadenopathy ($1.06 \pm 0.3 \times 10^{-3}\,mm^2/s$) (Fig. 4) is significantly lower ($P = 0.001$) than that of benign lymphadenopathy ($2.39 \pm 0.7 \times 10^{-3}\,mm^2/s$) at a *b* value of 0 and $600\,mm^2/s$. The optimal threshold of the ADC value is $1.85 \times 10^{-3}\,mm^2/s$ with an accuracy of 83.9% and sensitivity of 96.4%[44]. A potential problem when using diffusion MR imaging for mediastinal imaging may be the correct location of the lymph nodes because of the intrinsic low spatial resolution of diffusion MR imaging sequences. The use of fusion software allows for the overlaying of anatomic and diffusion MR imaging sequences, partially solving this problem[13].

Pleural mesothelioma

A preliminary study discussed the role of diffusion MR imaging in the characterization of pleural mesothelioma using a *b* value of $500/750\,mm^2/s$. The ADC values of epithelioid mesothelioma were statistically significantly ($P < 0.05$) greater than those of sarcomatoid mesothelioma. There was no significant difference between the ADC values of biphasic and sarcomatoid mesothelioma. This difference could serve as a surrogate imaging biomarker[45]. Also, the ADC value of transudate ($3.42–3.7 \times 10^{-3}\,mm^2/s$) is significantly different ($P = 0.01$) from that of exudate ($3.18–3.0 \times 10^{-3}\,mm^2/s$) at a *b* value of $1000\,mm^2/s$[46,47] (Fig. 4). Diffusion MR imaging is a promising tool for differentiating malignant pleural disease from benign lesions, with high accuracy, and supplementation with dynamic contrast-enhanced MR imaging seems to further improve sensitivity[48].

Future directions

Diffusion MR imaging can differentiate between viable and necrotic areas within head and neck tumors[49]. It has the potential to help select optimal biopsy sites and to detect the presence of viable tumors on follow-up studies

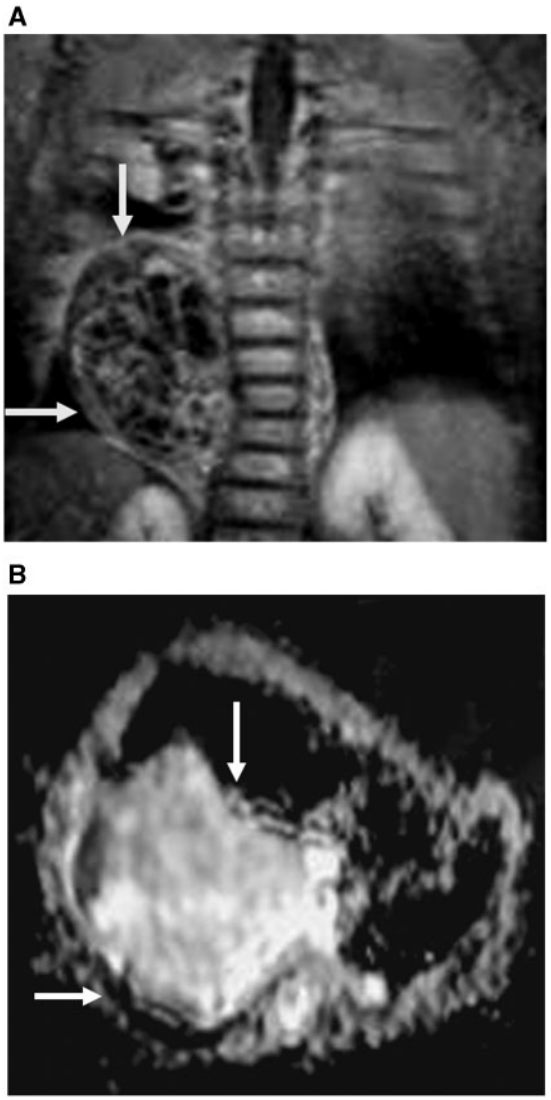

Figure 3 **Benign mediastinal mass. (A) Coronal contrast T1-weighted image shows large mass with multiple enhanced septae (arrows). (B) ADC map shows free diffusion of the mass (arrows) with a high ADC value (2.89×10^{-3} mm^2/s).**

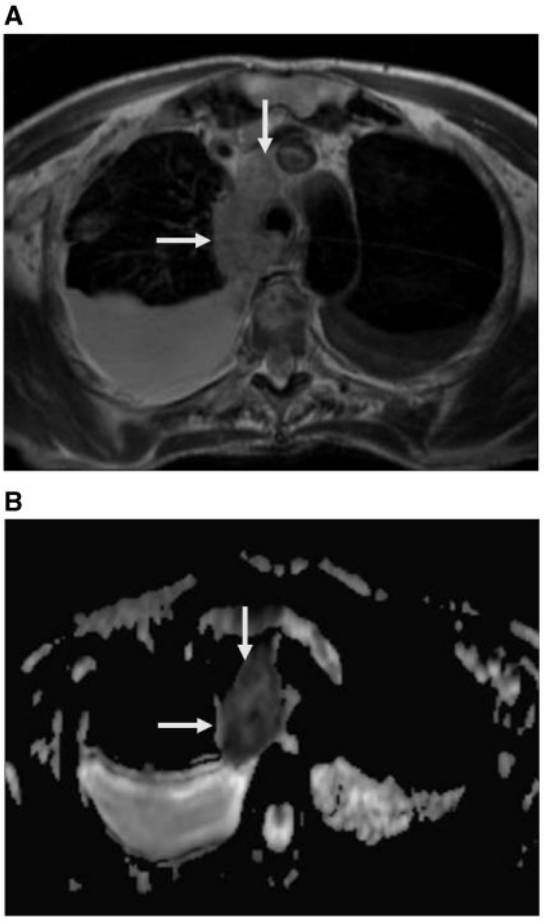

Figure 4 **Mediastinal lymphoma. (A) Axial true FISP shows enlarged right-sided mediastinal lymph node (arrows) with bilateral pleural effusion. (B) ADC map shows restricted diffusion with low ADC values (1.23×10^{-3} mm^2/s) of the mediastinal node (arrows). The pleural effusion shows high ADC values (3.22×10^{-3} mm^2/s on the right side and 2.98×10^{-3} mm^2/s on the left side.**

of patients who have undergone radiation therapy or chemotherapy. Studies are recommended to evaluate the role of diffusion MR imaging in the differentiation of cystic lung cancer from lung abscesses and in the assessment of chest wall, mediastinal, pericardial and cardiac invasion by lung cancer. Studies of the characterization of small pulmonary nodules and small nodal metastases are also recommended.

The application of new methods for data post-processing, such as diffusional non-Gaussian (kurtosis) modeling to fit diffusion-weighted imaging data acquired using an extended *b* value range or a K-means clustering algorithm that generates partitions of large datasets, may provide better characterization of lung cancer and may be of additional benefit in distinguishing benign and malignant pathologies compared with whole-lesion mean ADC alone[50].

Advantages

Diffusion MR imaging is a non-invasive functional imaging technique with acquisition times usually up to 4–6 min, depending on the slice coverage, amount of excitations, and amount of *b* values and, hence, adds little to the duration of the examination. Diffusion MR imaging is sensitive enough for the detection of pulmonary nodules, the differentiation of malignant from benign pulmonary masses and the staging of lung cancer. In addition, there is no exposure to ionizing radiation, and no need for administration of external tracer or contrast medium. Diffusion MR imaging can be

incorporated into routine morphological MR imaging to improve radiologist confidence in image interpretation and to provide functional assessments of chest lesions during the same examination[14,15].

Disadvantages

There are few limitations to the technique that must be resolved before increased widespread clinical application of diffusion MR imaging of the chest. The ADC value is a relative measure and not an absolute quantitative measure because the ADC depends on the *b* value and MR acquisition method used. Standardization of the acquisition parameters and post-processing methods between centers is needed. The ADC values vary widely for the same cancer subtype, with broad overlapping of the ADC values between benign and malignant tumors, in contradiction to its high sensitivity and accuracy. There is a need for intensive research studies with pathologic confirmation to validate the ADC value against known cancer pathologies to realize the full promise of the diffusion MR imaging approach. There is also a need for improvement in image quality, for example, by using parallel imaging, multichannel coils and higher field strengths (e.g., 3 T)[15–22].

Conclusion

Diffusion MR imaging offers functional imaging of lung cancer due to its ability to probe the tumoral microstructure, which is complementary to routine anatomic MR imaging of the chest. The potential value of diffusion MR imaging is in its detection, characterization, grading and staging of lung cancer. In addition, it has been used for the diagnosis and characterization of mediastinal and pleural tumors. It can be obtained in a short time without injection of contrast medium. The gradual development and standardization of imaging sequences and widespread research will make diffusion MR imaging of the chest more suitable for clinical applications in the future.

Acknowledgments

No funding was received for this study. Presented as an educational exhibit at the Assembly and Annual Meeting of the Radiological Society of North America (RSNA).

References

[1] Katz S, Ferrara T, Alavi A, et al. PET, CT, and MR imaging for assessment of thoracic malignancy: structure meets function. PET Clin 2009; 3: 395–410. doi:10.1016/j.cpet.2009.03.008.

[2] Shim SS, Lee KS, Kim BT, et al. Accuracy of integrated PET/CT using fluorodeoxyglucose for the preoperative staging of non-small cell lung cancer: a prospective comparison with standalone CT. Radiology 2005; 236: 1011–1019. doi:10.1148/radiol.2363041310. PMid:16014441.

[3] Hochhegger B, Marchiori E, Sedlaczek O, et al. MRI in lung cancer: a pictorial essay. Br J Radiol 2011; 84: 661–668. doi:10.1259/bjr/24661484. PMid:21697415.

[4] Bellomi M. Non-conventional imaging of lung cancer. Cancer Imaging 2010; 10: S161–162. doi:10.1102/1470-7330.2010.9035. PMid:20880776.

[5] Kauczor HU, Ley S. Thoracic magnetic resonance imaging 1985 to 2010. J Thorac Imaging 2010; 25: 34–38. doi:10.1097/RTI.0b013e3181cc4cd7. PMid:20160600.

[6] Rangel C, Cruz L, Jr. Takayassu T, Gasparetto E, Domingues R. Diffusion MR imaging in central nervous system. Magn Reson Imaging Clin North Am 2011; 19: 23–53. doi:10.1016/j.mric.2010.10.006.

[7] Malayeri A, El Khouli R, Zaheer A, et al. Principles and applications of diffusion-weighted imaging in cancer detection, staging, and treatment follow-up. Radiographics 2011; 31: 1773–1791. doi:10.1148/rg.316115515.

[8] Bonekamp S, Corona-Villalobos C, Kamel I. Oncologic applications of diffusion-weighted MRI in the body. J Magn Reson Imaging 2012; 35: 257–279. doi:10.1002/jmri.22786. PMid:22271274.

[9] Abdel Razek A. Diffusion-weighted magnetic resonance imaging of head and neck. J Comput Assist Tomogr 2010; 34: 808–815. doi:10.1097/RCT.0b013e3181f01796.

[10] Abdel Razek A, Gaballa G, Denewer A, Tawakol I. Diffusion weighted MR imaging of the breast. Acad Radiol 2010; 17: 382–386. doi:10.1016/j.acra.2009.10.014. PMid:20004597.

[11] Luna A, Sánchez-Gonzalez J, Caro P. Diffusion-weighted imaging of the chest. Magn Reson Imaging Clin North Am 2011; 19: 69–94. doi:10.1016/j.mric.2010.09.006.

[12] Luna A, Martin T, Sánchez-Gonzalez J. Diffusion-weighted imaging in the evaluation of lung, mediastinum, heart, and chest wall. In: Luna A, Ribes R, Soto JA, editors. Diffusion MRI outside the brain. Berlin: Springer-Verlag; 2012, p. 279–316.

[13] Henzler T, Schmid-Bindert G, Schoenberg SO, Fink C. Diffusion and perfusion MRI of the lung and mediastinum. Eur J Radiol 2010; 76: 329–336. doi:10.1016/j.ejrad.2010.05.005. PMid:20627435.

[14] Regier M, Schwarz D, Henes F, et al. Diffusion-weighted MR-imaging for the detection of pulmonary nodules at 1.5 Tesla: intraindividual comparison with multidetector computed tomography. J Med Imaging Radiat Oncol 2011; 55: 266–274. doi:10.1111/j.1754-9485.2011.02263.x. PMid:21696559.

[15] Matoba M, Tonami H, Kondou T, et al. Lung carcinoma: diffusion weighted MR imaging–preliminary evaluation with apparent diffusion coefficient. Radiology 2007; 243: 570–577. doi:10.1148/radiol.2432060131. PMid:17400757.

[16] Liu H, Liu Y, Yu T, Ye N. Usefulness of diffusion-weighted MR imaging in the evaluation of pulmonary lesions. Eur Radiol 2010; 20: 807–815. doi:10.1007/s00330-009-1629-6. PMid:19862533.

[17] Satoh S, Kitazume Y, Ohdama S, Kimula Y, Taura S, Endo Y. Can malignant and benign pulmonary nodules be differentiated with diffusion-weighted MRI? Am J Roentgenol 2008; 191: 464–470. doi:10.2214/AJR.07.3133.

[18] Mori T, Nomori H, Ikeda K, et al. Diffusion-weighted magnetic resonance imaging for diagnosing malignant pulmonary nodules/masses. Comparison with positron emission tomography. J Thorac Oncol 2008; 3: 358–364. doi:10.1097/JTO.0b013e318168d9ed. PMid:18379353.

[19] Uto T, Takehara Y, Nakamura Y, et al. Higher sensitivity and specificity for diffusion-weighted imaging of malignant lung lesions without apparent diffusion coefficient quantification. Radiology 2009; 252: 247–254. doi:10.1148/radiol.2521081195. PMid:19420317.

[20] Tondo F, Saponaro A, Stecco A, et al. Role of diffusion-weighted imaging in the differential diagnosis of benign and malignant lesions of the chest–mediastinum. Radiol Med 2011; 116: 720–733. doi:10.1007/s11547-011-0629-1. PMid:21293944.

[21] Chen W, Jian W, Li H, et al. Whole-body diffusion weighted imaging vs. FDG-PET for the detection of non-small-cell lung cancer. How do they measure up? Magn Reson Imaging 2010; 28: 613–620. doi:10.1016/j.mri.2010.02.009. PMid:20418042.

[22] Ohba Y, Nomori H, Mori T, et al. Is diffusion-weighted magnetic resonance imaging superior to positron emission tomography with fludeoxyglucose F 18 in imaging non–small cell lung cancer? J Thorac Cardiovasc Surg 2009; 138: 439–445. doi:10.1016/j.jtcvs.2008.12.026. PMid:19619793.

[23] Tanaka R, Horikoshi H, Nakazato Y, et al. Magnetic resonance imaging in peripheral lung adenocarcinoma: correlation with histopathologic features. J Thorac Imaging 2009; 24: 4–9. doi:10.1097/RTI.0b013e31818703b7. PMid:19242296.

[24] Koyama H, Ohno Y, Aoyama N, et al. Comparison of STIR turbo SE imaging and diffusion-weighted imaging of the lung: capability for detection and subtype classification of pulmonary adenocarcinomas. Eur Radiol 2010; 20: 790–800. doi:10.1007/s00330-009-1615-z. PMid:19763578.

[25] Kanauchi N, Oizumi H, Honma T, et al. Role of diffusion-weighted magnetic resonance imaging for predicting of tumor invasiveness for clinical stage IA non-small cell lung cancer. Eur J Cardiothorac Surg 2009; 35: 706–711. doi:10.1016/j.ejcts.2008.12.039. PMid:19216085.

[26] Abdel Razek A, Fathy A, Abdel Gawad T. Correlation of apparent diffusion coefficient value with prognostic parameters of lung cancer. J Comput Assist Tomogr 2011; 35: 248–252. doi:10.1097/RCT.0b013e31820ccf73.

[27] Regier M, Derlin T, Schwarz D, et al. Diffusion weighted MRI and 18F-FDG PET/CT in non-small cell lung cancer (NSCLC): Does the apparent diffusion coefficient (ADC) correlate with tracer uptake (SUV)? Eur J Radiol 2012; 81: 2913–2918. doi:10.1016/j.ejrad.2011.11.050. PMid:22197090.

[28] Baysal T, Mutlu D, Yologlu S. Diffusion-weighted magnetic resonance imaging in differentiation of postobstructive consolidation from central lung carcinoma. Magn Reson Imaging 2009; 27: 1447–1454. doi:10.1016/j.mri.2009.05.024. PMid:19553048.

[29] Qi L, Zhang X, Tang L, et al. Using diffusion-weighted MR imaging for tumor detection in the collapsed lung: a preliminary study. Eur Radiol 2009; 19: 333–341. doi:10.1007/s00330-008-1134-3. PMid:18690450.

[30] Nomori H, Mori T, Ikeda K, et al. Diffusion-weighted magnetic resonance imaging can be used in place of positron emission tomography for N staging of non-small cell lung cancer with fewer false-positive results. J Thorac Cardiovasc Surg 2008; 135: 816–822. doi:10.1016/j.jtcvs.2007.10.035. PMid:18374761.

[31] Hasegawa I, Boiselle P, Kuwabara K, Sawafuji M, Sugiura H. Mediastinal lymph nodes in patients with non-small cell lung cancer: preliminary experience with diffusion-weighted MR imaging. J Thorac Imaging 2008; 23: 157–161. doi:10.1097/RTI.0b013e318166d2f5. PMid:18728541.

[32] Nakayama J, Miyasaka K, Omatsu T, et al. Metastases in mediastinal and hilar lymph nodes in patients with non-small cell lung cancer: quantitative assessment with diffusion-weighted magnetic resonance imaging and apparent diffusion coefficient. J Comput Assist Tomogr 2010; 34: 1–8. doi:10.1097/RCT.0b013e3181a9cc07. PMid:20118713.

[33] Pauls S, Schmidt S, Juchems M, et al. Diffusion-weighted MR imaging in comparison to integrated [^{18}F]-FDG PET/CT for N-staging in patients with lung cancer. Eur J Radiol 2012; 81: 178–182. doi:10.1016/j.ejrad.2010.09.001. PMid:20932700.

[34] Ohno Y, Koyama H, Yoshikawa T, et al. N stage disease in patients with non-small cell lung cancer: efficacy of quantitative and qualitative assessment with STIR turbo spin-echo imaging, diffusion-weighted MR imaging, and fluorodeoxyglucose PET/CT. Radiology 2011; 261: 605–615. doi:10.1148/radiol.11110281. PMid:21926377.

[35] Ohno Y, Koyama H, Onishi Y, et al. Non–small cell lung cancer: whole-body MR examination for M-stage assessment–utility for whole-body diffusion-weighted imaging compared with integrated FDG PET/CT. Radiology 2008; 248: 643–654. doi:10.1148/radiol.2482072039. PMid:18539889.

[36] Takenaka D, Ohno Y, Matsumoto K, et al. Detection of bone metastases in non-small cell lung cancer patients: comparison of whole-body diffusion-weighted imaging (DWI), whole-body MR imaging without and with DWI, whole-body FDGPET/CT, and bone scintigraphy. J Magn Reson Imaging 2009; 30: 298–308. doi:10.1002/jmri.21858. PMid:19629984.

[37] Okuma T, Matsuoka T, Yamamoto A, et al. Assessment of early treatment response after CT-guided radiofrequency ablation of unresectable lung tumours by diffusion-weighted MRI: a pilot study. Br J Radiol 2009; 82: 989–994. doi:10.1259/bjr/13217618. PMid:19470575.

[38] Yabuuchi H, Hatakenaka M, Takayama K, et al. Non-small cell lung cancer: detection of early response to chemotherapy by using contrast-enhanced dynamic and diffusion-weighted MR imaging. Radiology 2011; 261: 598–604. doi:10.1148/radiol.11101503. PMid:21852569.

[39] Ohno Y, Koyama H, Yoshikawa T, et al. Diffusion-weighted MRI versus ^{18}F-FDG PET/CT: performance as predictors of tumor treatment response and patient survival in patients with non-small cell lung cancer receiving chemoradiotherapy. Am J Roentgenol 2012; 198: 75–82. doi:10.2214/AJR.11.6525.

[40] Abdel Razek A, Elmorsy A, Elshafey M, Elhadedy T, Hamza O. Assessment of mediastinal tumors with diffusion weighted single shot echo planar MR imaging. J Magn Reson Imaging 2009; 30: 535–540. doi:10.1002/jmri.21871.

[41] Gümüştaş S, İnan N, Sarisoy H, et al. Malignant versus benign mediastinal lesions: quantitative assessment with diffusion weighted MR imaging. Eur Radiol 2011; 21: 2255–2260.

[42] Abdel Razek A, Soliman N, Elashery R. Apparent diffusion coefficient values of mediastinal masses in children. Eur J Radiol 2012; 81: 1311–1314. doi:10.1016/j.ejrad.2011.03.008. PMid:21439745.

[43] Kosucu P, Tekinbas C, Erol M, et al. Mediastinal lymph nodes: assessment with diffusion-weighted MR imaging. J Magn Reson Imaging 2009; 30: 292–297. doi:10.1002/jmri.21850. PMid:19629990.

[44] Abdel Razek A, Elkammary S, Elmorsy A, et al. Characterization of mediastinal lymphadenopathy with diffusion-weighted imaging. Magn Reson Imaging 2011; 29: 167–172. doi:10.1016/j.mri.2010.08.002. PMid:20951522.

[45] Gill R, Umeoka S, Mamata H, et al. Diffusion-weighted MRI of malignant pleural mesothelioma: preliminary assessment of apparent diffusion coefficient in histologic subtypes. Am J Roentegonl 2010; 195: W125–130. doi:10.2214/AJR.09.3519.

[46] Baysal T, Bulut T, Gökirmak M, Kalkan S, Dusak A, Dogan M. Diffusion-weighted MR imaging of pleural fluid: differentiation of transudative vs exudative pleural effusions. Eur Radiol 2004; 14: 890–896. PMid:12904883.

[47] Inan N, Arslan A, Akansel G, et al. Diffusion weighted MRI in the characterization of pleural effusions. Diagn Interv Radiol 2009; 15: 13–18. PMid:19263368.

[48] Coolen J, De Keyzer F, Nafteux P, et al. Malignant pleural disease: diagnosis by using diffusion-weighted and dynamic contrast-enhanced MR imaging–initial experience. Radiology 2012; 263: 884–892. doi:10.1148/radiol.12110872. PMid:22535562.

[49] Abdel Razek A, Megahed A, Motamed A, Tawfik A, Nada N. Role of diffusion weighted MR imaging in differentiation between viable and necrotic part of head and neck tumors. Acta Radiol 2008; 49: 364–370. doi:10.1080/02841850701777390.

[50] Schafer J, Srinivasan A, Mukherji S. Diffusion magnetic resonance imaging in the head and neck. Magn Reson Imaging Clin North Am 2011; 19: 55–67. doi:10.1016/j.mric.2010.10.002.